Journal of Macromolecular Science, Part A
Publication details, including instructions for authors and subscription information:
http://www.informaworld.com/smpp/title~content=t713597274

Plasma Polymerization on Metals

P. J. Dynes[a]; D. H. Kaelble[a]
[a] Science Center Rockwell International Thousand, Oaks, California

To cite this Article Dynes, P. J. and Kaelble, D. H.(1976) 'Plasma Polymerization on Metals', Journal of Macromolecular Science, Part A, 10: 3, 535 — 557
To link to this Article: DOI: 10.1080/00222337608061198
URL: http://dx.doi.org/10.1080/00222337608061198

J. MACROMOL. SCI.—CHEM., A10(3), pp. 535-557 (1976)

Plasma Polymerization on Metals

P. J. DYNES and D. H. KAELBLE

Science Center
Rockwell International
Thousand Oaks, California 91360

ABSTRACT

An ellipsometric technique is described for accurately measuring the film thickness of plasma-polymerized polymers on metallic substrates. The index of refraction n and absorption index κ of the plasma polymer film can also be studied by ellipsometry. Films of plasma polystyrene and polyepichlorohydrin were deposited on evaporated aluminum substrates and their thickness and optical constants determined. Plasma polystyrene films from 20 to 1600 Å thick have optical constants $n = 1.63$ and $\kappa = 0$ independent of film thickness. Plasma polyepichlorohydrin films over the same range of thickness give $n \simeq 1.70$ and $\kappa \simeq 0.01$. By utilizing the ellipsometric method the effect of plasma polymer film thickness on surface energy properties was determined. Advancing contact angle measurements and surface energy analysis detail the polar γ_{SV}^{p} and dispersion γ_{SV}^{d} contributions to the solid-vapor surface tension $\gamma_{SV} = \gamma_{SV}^{d} + \gamma_{SV}^{p}$ of plasma polystyrene and polyepichlorohydrin films on etched aluminum. For thin plasma polystyrene films (<600 Å), anomalies in the

calculated surface energy are discussed and related to possible surface nonuniformity caused by film growth. Thicker films of plasma polystyrene are shown to have normal surface energy properties as does plasma polyepichlorohydrin over the entire range of film thickness measured. The adhesive and cohesive properties of plasma polystyrene and polyepichlorohydrin films are discussed as estimated from a lap-shear bond strength study. Etched aluminum coated with various thicknesses of these two polymers and bonded with an epoxy-phenolic adhesive shows a decreasing shear strength with increasing plasma film thickness but begins to level off at ~1600 psi for films >1600 Å thick.

INTRODUCTION

The polymerization of organic and inorganic monomer vapors in a rf glow discharge has become an important technique in the development of new polymeric materials [1-6]. The most significant characteristic of plasma-polymerized polymers is their ability to provide useful functions when deposited on substrates as thin continuous films (~10^2 to 10^4 Å). The accurate measurement of film thickness in this range, however, is difficult by conventional means such as the profilometer method, capacitance measurements, or interferometry. In the present investigation an ellipsometric technique is described for the accurate determination of the thickness of plasma-polymerized films deposited on metallic substrates. Ellipsometric analysis can in addition provide information concerning the refractive index n and absorption index κ of these films.

In many of the technological applications of these materials, such as reverse osmosis membranes [3, 7] and protective coatings [2], a knowledge of wettability properties can provide valuable information relating to their permeability and adhesion behavior. No studies, however, appear to have been made detailing the surface energy character of any of these polymers. We have, therefore, measured contact angles for a series of test liquids on two plasma polymers deposited on an aluminum substrate to various film thicknesses. From a two-parameter model [8] for liquid-solid interactions the polar and dispersion contributions to the solid-vapor surface tension of the polymer film are isolated. Anomalous values of the surface energy for films thinner than ~600 Å may be related to the results of recent studies [5, 9, 10] which show both substrate topology and plasma discharge conditions affect the morphology of plasma-polymerized films.

As the final objective of this study, the adhesive and cohesive strengths of plasma-polymerized films on aluminum are evaluated from a lap-shear bond strength study.

EXPERIMENTAL

Plasma System and Materials

In the present study an inductively coupled electrodeless plasma system was used and is shown schematically in Fig. 1. The rf power supply is a modified Trapelo PDS 302 (LFE Corp.). This unit operates at 13.56 MHz and provides a variable output power from 0 to 200 W. The impedance match between the rf generator and load is optimized by an automatic tuning mechanism which maintains the reflected power at a minimum.

Prior to introduction of the monomer, the reaction chamber was pumped down to ~1 μmHg. A needle valve on the monomer reservior was used to control the pressure as measured by a pressure transducer (MKS Baratron). To allow the system to attain a steady pressure, the plasma chamber was purged for ~10 min before initiation of the plasma. More uniform polymerization has been reported [11] without the use of a carrier gas, and none was used in this study.

Substrates were aluminum Al 2024-T3 alloy and evaporated aluminum on glass. Evaporated aluminum mirrors were prepared by evaporating onto a polished glass surface in vacuum, first chromium, then gold, and finally a film of aluminum. By this procedure the aluminum adheres well and is very smooth, permitting accurate ellipsometric measurements to be made.

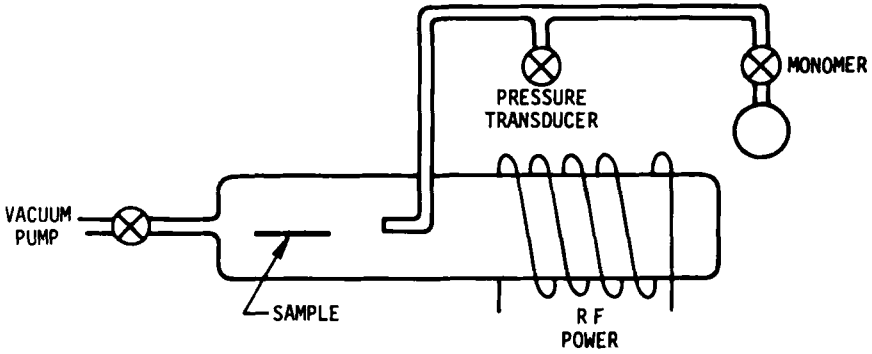

FIG. 1. Schematic diagram of rf discharge system.

The second substrate was rolled, 0.16 cm thick Al 2024-T3 (Ducommun Metal and Supply Co., Los Angeles) which represents a common aluminum alloy used in structural applications. This material was given the standard FPL (Forest Products Laboratory) [12] surface treatment prior to its use as a substrate. Briefly, this treatment consists of a solvent and alkaline cleaning followed by a sulfuric acid-dichromate etch. After rinsing with distilled water and drying at 23°C, the samples were used within 2 hr. Substrates were plasma-polymer coated in the reaction chamber at a fixed point 2 in. downstream from the monomer inlet and 6 in from the rf coils in the after-glow region of the plasma. Operating in this region away from the rf coils minimizes inductive heating of the metallic substrates and results in slower and more uniform polymerization. Monomers used were styrene (Aldrich), dried with activated alumina, and epichlorohydrin (Eastman Organic Chemicals), used without further purification.

Ellipsometry

The theory and experimental technique used in ellipsometric measurements has been given by several authors [13-15]. In brief, the method is based on the fact that when a beam of plane polarized light is reflected from a metallic surface, the reflected light becomes elliptically polarized. This results in a relative phase shift (Δ) in the normal and parallel components of the polarized light beam, and a change in the ratio of their relative amplitude attenuation ($\tan \psi$). These two parameters are the common experimental variables measured in ellipsometry. Other parameters associated with ellipsometric measurements are the angle of incidence of the light beam to the sample and the wavelength of the light. From an analysis based on classical optics, equations have been derived relating Δ and ψ together with the wavelength and angle of incidence to the refractive index n and absorption index κ of the metallic substrate where the complex refractive index of an absorbing medium is defined as $\hat{n} = n(1 - i\kappa)$ with $i = \sqrt{-1}$. In addition, the analysis can be extended to calculate the optical constants η and κ and thickness d of any surface films present on the metallic substrate. To solve the complex equations which result from such an analysis, a computer program has been developed by McCrackin [16] and was used in this study.

The experimental optical arrangement of the commercial (O. C. Rudolph & Sons, Inc.) ellipsometer is shown schematically in Fig. 2. A monochromatic beam of light of ~2 mm diameter from a He-Ne laser whose wavelength is 6328 Å is first polarized and then compensated with a quarter-wave plate (compensator).

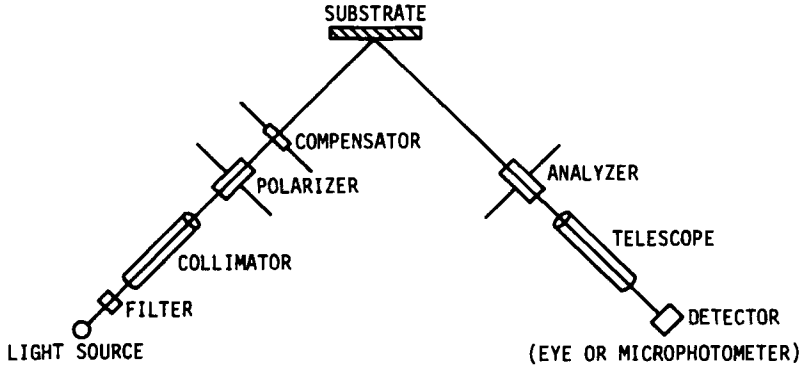

FIG. 2. Schematic representation of the optical arrangement of the ellipsometer.

The light beam then strikes the sample at an angle of incidence of 70° and passes into an analyzer and finally into a photometer detector. It can be shown that if the polarizer and analyzer are rotated until a minimum in light intensity is registered, then the azimuths of the polarizer (p) and analyzer (a) permit direct calculation of Δ and ψ; $\Delta = 2p + \pi/2$ and $\psi = a$. Measurement of p and a to ±0.01° for four quadrants or zones related to the polarizer, analyzer, and compensator angles were averaged to minimize alignment errors [13]. Values of Δ and ψ obtained in this way were then put into the McCrackin program with the wavelength of light (6328 Å) and angle of incidence (70°) to obtain film thicknesses and optical properties.

Wettability

Advancing contact angle measurements were made by the sessile-drop method at 23°C using an NRL goniometer (Rame-Hart, Inc.). The test liquids and their surface tension properties are listed in Table 1. The contact angle data was analyzed according to a surface energy model developed by Kaelble [8] to isolate the separate (London-d) dispersion and (Keesom-p) polar contributions to the solid-vapor surface tension. This analysis technique, which has been detailed previously [17, 18], is summarized in Eqs. (1) to (5):

$$\gamma_{LV} = \gamma_{LV}^{d} + \gamma_{LV}^{p} = \alpha_L^2 + \beta_L^2 \tag{1}$$

TABLE 1. Surface Tension Properties of Test Liquids at 20°C

Test liquid	γ_{LV} (dyn/cm)	γ_{LV}^{d} (dyn/cm)	γ_{LV}^{p} (dyn/cm)	$2\alpha_L$ $(dyn/cm)^{1/2}$	β_L/α_L
Water	72.8	21.8	51.0	9.34	1.53
Glycerol	64.0	34.0	30.0	11.66	0.94
Formamide	58.3	32.3	26.0	11.37	0.90
Ethylene glycol	48.3	29.3	19.0	10.83	0.81
1-Bromonapthalene	44.6	44.6	0.0	13.36	0.00
Glycol PG-E-200	43.5	28.2	15.3	10.62	0.74
Tricresyl phosphate	40.9	39.2	1.7	12.52	0.21
Glycol PG-15-200	36.6	26.0	10.6	10.20	0.64
Glycol PG-1200	31.3	24.5	6.8	9.90	0.53
n-Hexadecane	27.6	27.6	0.0	10.51	0.00

$$\gamma_{SV} = \gamma_{SV}^{d} + \gamma_{SV}^{p} = \alpha_S^2 + \beta_S^2 \tag{2}$$

$$W_a = \gamma_{LV}(1 + \cos\theta) \leq 2\gamma_{LV} \tag{3}$$

$$W_a = 2[\alpha_L\alpha_S + \beta_L\beta_S] = W_a^{d} + W_a^{p} \tag{4}$$

$$W_a/2\alpha_L = \alpha_S + \beta_S(\beta_L/\alpha_L) \tag{5}$$

where γ_{LV} = liquid-vapor surface tension
γ_{SV} = solid-vapor surface tension
α_L, β_L = square root of the respective (London) dispersion γ_{LV}^{d} and (Keesom) polar γ_{LV}^{p} parts of γ_{LV}
α_S, β_S = square roots of respective dispersion γ_{SV}^{d} and polar γ_{SV}^{p} parts of γ_{SV}
W_a = nominal work of adhesion
θ = liquid-solid contact angle

The analysis involves calculating the work of adhesion from the experimental contact angle using Eq. (3) and substituting it into Eq. (4) where α_L and β_L are known from literature values of γ_{LV}^{d} and γ_{LV}^{p}. The unknown surface components for the solid $\alpha_S = (\gamma_{SV}^{d})^{1/2}$ and $\beta_S = (\gamma_{SV}^{p})^{1/2}$ are computed from Eq. (4) using a computerized determinant analysis [17] or graphically from Eq. (5) where a plot of $W_a/2\alpha_L$ vs β_L/α_L yields α_S as the intercept and whose slope is β_S

Tensile Lap-Shear Bonds

Adhesive bonds were prepared from 1 × 4 in. coupons of 0.16 cm thick Al 2024-T3 and HT-424 epoxy-phenolic adhesive (American Cyanamid Company). This adhesive contains aluminum powder filler and is supported on a glass fabric carrier. The aluminum coupons were first given the FPL etch treatment and then exposed to a styrene or epichlorohydrin plasma to give the desired plasma polymer film thickness. In this way the plasma polymer film

replaces the usual primer coating applied to protect the freshly etched aluminum. A 1 × 1/2 in. section of film adhesive was then applied to one end of a plasma-polymer-coated coupon and another coupon placed on top to complete the overlap bond. Alignment and an exactly 0.500 in. overlap are maintained by a special bonding fixture. This fixture, containing up to six bonds, was then placed in a heated press at ~50 psi and the adhesive cured at 166°C for 1 hr. Bonds were sheared at a crosshead rate of 0.01 in./min using an Instron floor model testing machine where stress in pounds vs strain is recorded. The tensile shear strength of three bonds was averaged for each plasma polymer coating thickness tested.

RESULTS AND DISCUSSION

The surface model used in the ellipsometric calculations is shown schematically in Fig. 3. To compute the properties of the polymer film, we must know the optical constants n and κ of aluminum metal and its naturally occurring oxide. The thickness d of this oxide layer must also be known. At a wavelength of 6328 Å, aluminum metal has an index of refraction of $n_3 \simeq 1.43$ and an absorption index of $\kappa_3 \simeq 5.17$. With this data and the experimental Δ and ψ values for the evaporated aluminum mirror without a polymer film, the computer program of McCrackin [16] can calculate the thickness and optical constants of the oxide layer. With three unknowns and just two independent experimental variables, this program can only compute sets of n_2, κ_2, and d_2 for given ranges of n_2 and κ_2. Bulk oxides of aluminum, however, are usually transparent ($\kappa = 0$) at a wavelength of 6328 Å, and their refractive index is known to be 1.5 to 1.8 [19]. Solutions can therefore be chosen with κ_2 and n_2 closest to these bulk values.

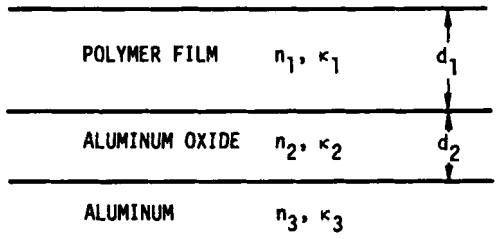

FIG. 3. Model of surface film structure used in ellipsometric analysis.

By using these criteria, the best solution for the oxide layer on evaporated aluminum gives $n_2 \simeq 1.70$, $\kappa \simeq 0.04$, and $d_2 \simeq 50$ Å. Some variation in these values is found from sample to sample and is believed to be related to the effect of surface roughness on ellipsometric parameters as discussed by Fenstermaker and McCrackin [20]. When this same approach is applied to calculate the properties of the oxide layer on FPL-etched AL 2024-T3, the best solution computed gives $n_2 \simeq 1.69$, $\kappa_2 \simeq 0.4$ and $d_2 \simeq 180$ Å. This high κ value may be the result of errors caused by the extreme surface roughness of this substrate. Knowing these properties for the two aluminum substrates now permits calculation of the thickness and optical constants of deposited plasma-polymerized films.

In Fig. 4 the variation of the experimental ellipsometric parameters Δ and ψ is given as a function of cumulative exposure time for an evaporated aluminum substrate to a styrene and epichlorohydrin plasma. For these measurements the substrate was exposed for a given interval of time to the plasma by the technique described previously and then removed from the plasma chamber and measurement of Δ and ψ made. This procedure was then repeated using the same substrate to build up a film as a function of cumulative plasma exposure time. In experiments both with styrene and epichlorohydrin the discharge was operated at a monomer vapor pressure of 140 μmHg and an rf power of 3 W. The experimental Δ and ψ pairs for each exposure time were then put into the McCrackin program together with the best solution for n_2, κ_2, and d_2 of the oxide substrate, and solutions searched over a range of polymer optical constants where $1.5 \leq n_1 \leq 2$ and $\kappa_1 \leq 0.1$.

The solutions found for the case of plasma polystyrene (PPS) all gave an absorption index of $\kappa_1 = 0$ and an average index of refraction of $n_1 = 1.63 \pm 0.02$. In Fig. 5 the computed film thickness values of these solutions are plotted vs cumulative plasma exposure time where a deposition rate of 50 Å/min is found. PPS thus illustrates the special case of a transparent ($\kappa = 0$) film whose index of refraction and thickness can be determined from Δ and ψ with less ambiguity. A disadvantage, however, is that for transparent films Δ and ψ are periodic functions of the film thickness. In Fig. 4 we find that one complete cycle has almost been completed at about 2200 Å for PPS. In the present work, films were grown slowly giving Δ-ψ values in cycle 1, thus permitting the elimination of computed solutions for higher cycles.

In Fig. 4 the experimental Δ-ψ curve for plasma polyepichlorohydrin (PPE) is seen to deviate widely from that of PPS. When solutions for these Δ-ψ pairs were computed, singular solutions with $\kappa_1 = 0$ and $n_1 \simeq 1.7$ were found for films <500 Å, but for thicker films a family of solutions of n_1, κ_1, and d_1 was computed.

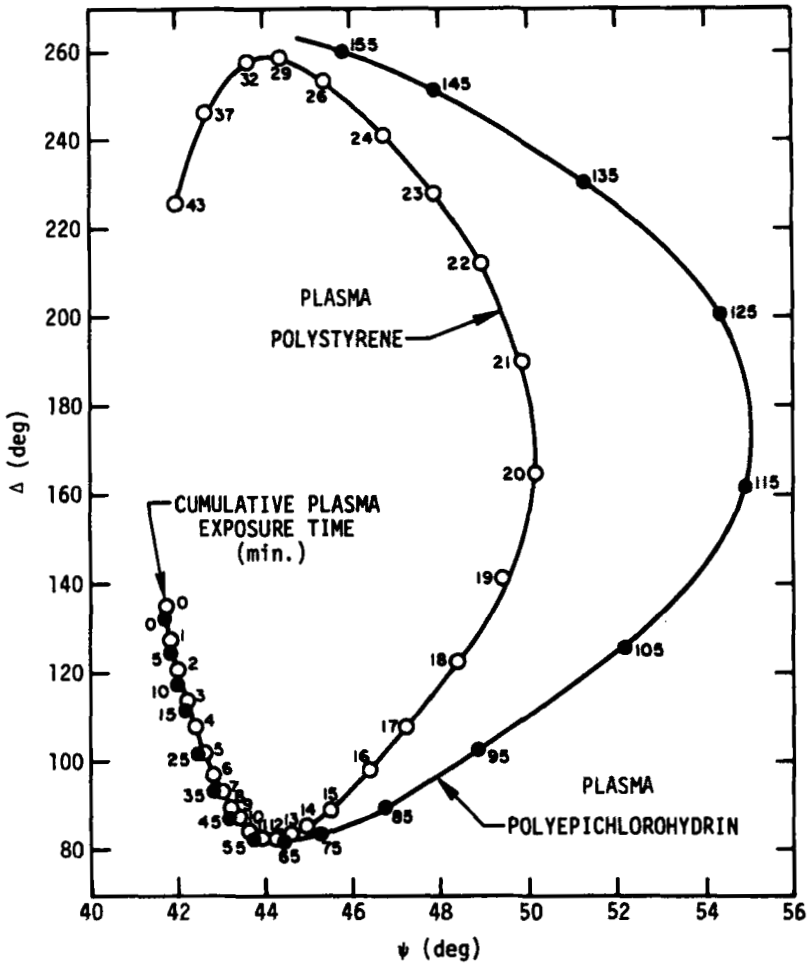

FIG. 4. Variation of the ellipsometric parameters Δ and ψ with cumulative plasma exposure time for plasma polystyrene and polyepichlorohydrin films on evaporated aluminum at 140 μmHg monomer pressure and 3 W rf power.

In contrast to PPS, PPE represents an example of an absorbing ($\kappa > 0$) film in which Δ and ψ are not sufficient to define the three film parameters. In most cases, however, for films of less than a few hundred angstroms, the calculated thickness values are relatively insensitive to n_1 or κ_1 values. This is shown in Fig. 4 where

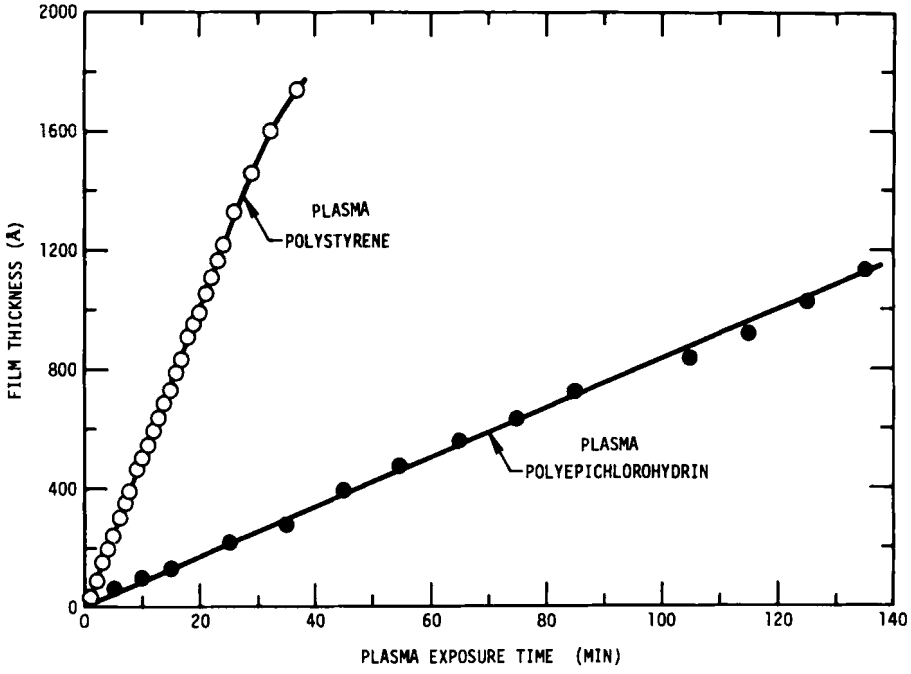

FIG. 5. Effect of cumulative plasma exposure time on growth of plasma polystyrene and polyepichlorohydrin films on evaporated aluminum at 140 μmHg monomer pressure and 3 W rf power.

the Δ-ψ curves for PPS and PPE nearly overlap for thin films while for thicker ones large differences are noted. The small deviation that is seen for thin films is mainly due to the initial difference between the two substrates. Therefore, using the solutions for thin films, an approximate deposition rate of 8.4 Å/min was calculated for PPE. From this deposition rate, approximate thickness values could then be determined from plasma exposure times for films >500 Å. These film thickness values were then used to select the best from among the multiple solutions given for these films. By this method an average index of refraction $n_1 \simeq 1.70$ and $\kappa_1 \simeq 0.01$ was found. In Fig. 5 PPE thickness values for films <500 Å are plotted vs cumulative plasma exposure time together with the values of those >500 Å selected by the above method.

For the case of plasma polymer films on FPL-etched alunimum, exact ellipsometric solutions could not be found due to inaccuracies in the calculated oxide properties for this substrate. Polymer film

thickness values can still be determined, however, from the McCrackin program by generating tables of Δ and ψ values as a function of film thickness using the previously calculated polymer optical constants and the approximate oxide substrate parameters. From these tables, relative film thickness values on FPL-etched aluminum were determined. With the same discharge parameters the rate of deposition of both plasma polymers was equal to that on evaporated aluminum. This technique for determining relative film thickness is very important because in many cases, like the above metal or oxide, properties are not known well enough to obtain exact ellipsometric solutions. It is also by this procedure that the real power of the ellipsometric technique can be utilized to measure relative film thickness changes with a precision of <1 Å.

Due to the greater sensitivity of the polymer optical constants to uncertainties in the metallic substrate properties, n_1 and κ_1 cannot be determined as accurately as film thickness. The calculated refractive index of 1.63 for PPS at 6328 Å is slightly higher than that of bulk polystyrene with n = 1.59 to 1.60 at 5893 Å [21]. Bui and co-workers [22], using an ac electrode-type discharge, have reported an index of 1.71 for PPS on evaporated gold using ellipsometry. A higher refractive index for plasma polystyrene would be expected on the basis of work by Knickmeyer and co-workers [23] who reported this material to be about 20% more dense than either amorphous or crystalline polystyrene. The index should also be increased by the large amount of oxygen with which plasma polymers tend to combine [23]. Elemental analysis of the plasma polystyrene produced in this study show it to contain 17.7% oxygen, 0.6% nitrogen, 75.7% carbon, and 6.2% hydrogen by weight.

The value of $\kappa = 0$ for PPS and $\kappa \approx 0.01$ for PPE are reasonable values for polymers at 6328 Å. Transmission of plasma polymers in the visible region is usually high but varies somewhat depending on the discharge conditions [2]. A κ of 0.01 for PPE corresponds to an absorption coefficient of 3×10^{-5}/Å.

In Fig. 5 a leveling off in the deposition of PPS is noted when the deposition time was increased beyond 1 min. This effect was investigated by measuring the rate of deposition as a function of deposition time, and the results are presented in Fig. 6 for both PPS and PPE. In these experiments the film thicknesses were determined by the technique described previously in which experimental Δ-ψ values are correlated with computer generated tables of Δ and ψ for varying film thicknesses. For polymerization times of less than ~ 5 min the deposition rate is seen to increase for both PPS and PPE. This effect was independent of the film thickness on the substrate or the order in which the

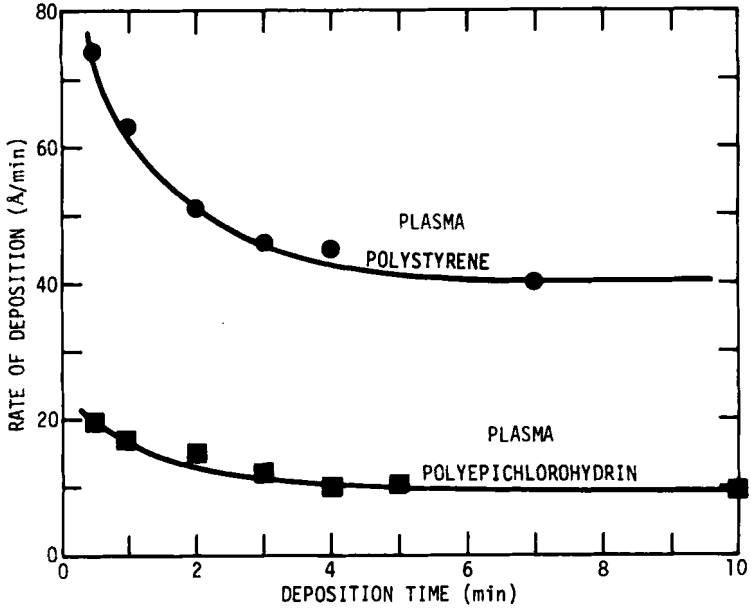

FIG. 6. Dependence of the rate of deposition on deposition time for plasma polystyrene and polyepichlorohydrin on evaporated aluminum at 170 μmHg monomer pressure and 3 W rf power.

deposition times were made. A similar finding has been reported by Connell and Gregor [24] for the plasma polymerization of divinylbenzene in a system where the thermal contact between a cooled substrate holder and sample was poor. When the thermal contact was made more efficient, only a small decrease in deposition rate with time was found. It is likely that this deposition rate decrease is due to desorption of monomer caused by an increase in the temperature of the substrate which takes a few minutes to equilibrate the plasma.

The effect of rf power on the rate of film growth on etched Al is shown in Fig. 7. At a constant steady flow pressure of 200 μmHg an approximately linear increase in deposition rate with input power was found. This effect, however, appears to be sensitive to where the deposition rate is measured in the chamber in relation to the rf coils. Using a similar experimental setup but with the rf coils apparently further removed from the sample than in the present study, Yasuda and Lamaze [11] found the deposition rate to be independent of discharge power. Thompson and Mayan [25], also using an electrodeless system, reported an increasing

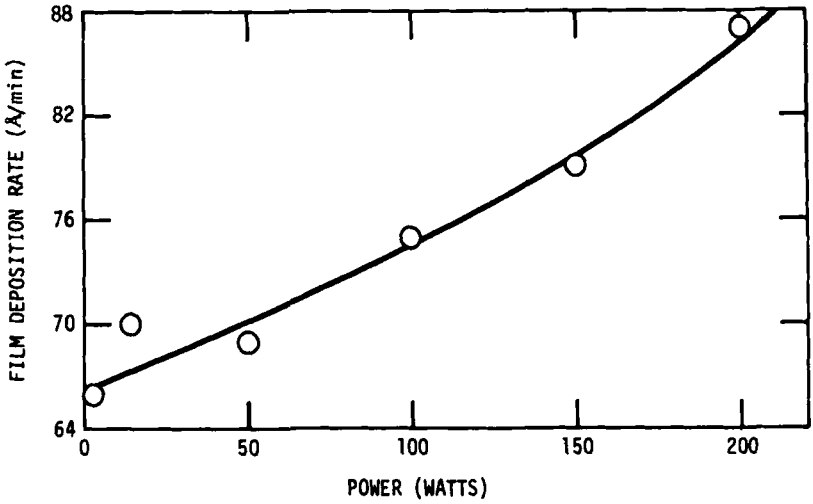

FIG. 7. Effect of rf power on the deposition rate of plasma polystyrene on FPL-etched Al 2024-T3 at 200 μmHg monomer pressure.

rate of polymerization with power which leveled off at about 30 W. In the latter study the rate of deposition was determined by weighing all the polymer formed in the system, most of which was deposited within the rf coil region.

Advancing contact angle measurements for nine test liquids on PPS and PPE films of various thickness are given in Tables 2 and 3. Films were grown on freshly FPL-etched Al 2024-T3 at 170 μmHg monomer pressure and 3 W rf power. The film thickness was calculated using previously established deposition rates. As seen in Tables 2 and 3, freshly FPL-etched Al 2024-T3 provides a surface on which all the test liquids display nearly zero contact angles. By starting with such a high-energy surface, the deposition of a lower energy polymer film is easier to detect by wettability measurements. This is evident in Tables 2 and 3 where large changes in contact angle occur for even very thin polymer coatings. No change in contact angle, however, was found by exposing fresh substrates to monomer vapor without a plasma.

In Fig. 8 determinant calculations of the polar γ_{SV}^{p} and dispersion γ_{SV}^{d} contributions to the total surface energy $\gamma_{SV} = \gamma_{SV}^{p} + \gamma_{SV}^{d}$ are given for the contact angle data of Tables 2 and 3. For thicker films (>600 Å) where the surface energy is independent of film thickness, we find for

TABLE 2. Advancing Contact Angle Measurements for Plasma-Polymerized Polystyrene Films on FPL-Etched Al-2024-T3

	Film thickness (Å)												
Test liquid	0	37	63	102	138	168	205	300	440	640	1000	1200	1600
Water	4	110	108	104	106	105	100	100	100	80	90	78	78
Glycerol	4	105	100	91	89	92	88	87	85	80	70	72	72
Formamide	7	90	74	61	55	59	65	51	57	52	52	50	54
Ethylene glycol	1	62	44	34	25	20	21	20	25	27	36	35	30
1-Bromonapthalene	2	2	9	5	5	5	5	5	4	5	6	7	6
Glycol PG-E-1200	5	41	10	5	4	5	5	8	7	5	8	11	10
Tricresyl phosphate	5	2	5	5	5	6	8	5	5	6	7	5	5
Glycol PG-15-200	5	15	13	12	15	15	10	10	10	15	15	16	15
Glycol PG-1200	6	10	8	5	5	5	10	10	10	10	10	10	10

TABLE 3. Advancing Contact Angle Measurements for Plasma-Polymerized Polyepichlorohydrin Films on FPL-Etched Al 2024-T3

Test liquid	Film thickness (Å)							
	0	17	50	200	400	600	800	1000
Water	14	53	66	64	65	68	63	64
Glycerol	12	70	87	77	74	70	68	69
Formamide	6	11	29	35	40	40	42	33
Ethylene glycol	3	30	31	40	36	33	39	37
1-Bromonapthalene	2	8	6	10	10	9	10	10
Glycol PG-E-200	7	16	7	5	8	12	7	6
Tricresyl phosphate	8	8	5	4	7	10	8	7
Glycol PG-15-200	9	10	8	6	9	9	5	4
Glycol PG-1200	5	7	6	5	7	5	3	2

PPS $\gamma_{SV}^{d} \simeq 37$ and $\gamma_{SV}^{p} \simeq 5$, giving a $\gamma_{SV} \simeq 42$ dyn/cm. For PPE $\gamma_{SV}^{d} \simeq 33$, $\gamma_{SV}^{p} \simeq 13$, and $\gamma_{SV} \simeq 44$ dyn/cm. The surface tension components for normal polystyrene are $\gamma_{SV}^{d} = 38.4$, $\gamma_{SV}^{p} = 2.2$, and $\gamma_{SV} = 40.6$ dyn/cm [17].

In Fig. 8 we note for films of PPS <600 Å that the dispersion component γ_{SV}^{d} increases substantially. This effect may be related to the surface topology exhibited by PPS on FPL-etched Al 2024-T3. In the present surface energy analysis it is assumed that the solid substrate is a smooth homogeneous plane. In this analysis by either the determinant method using Eq. (4) or graphically from Eq. (5), the value of the polar component β_s is computed and squared to yield the γ_{SV}^{p} values plotted in Fig. 8. Normally the value of β_s is positive but for these films it is

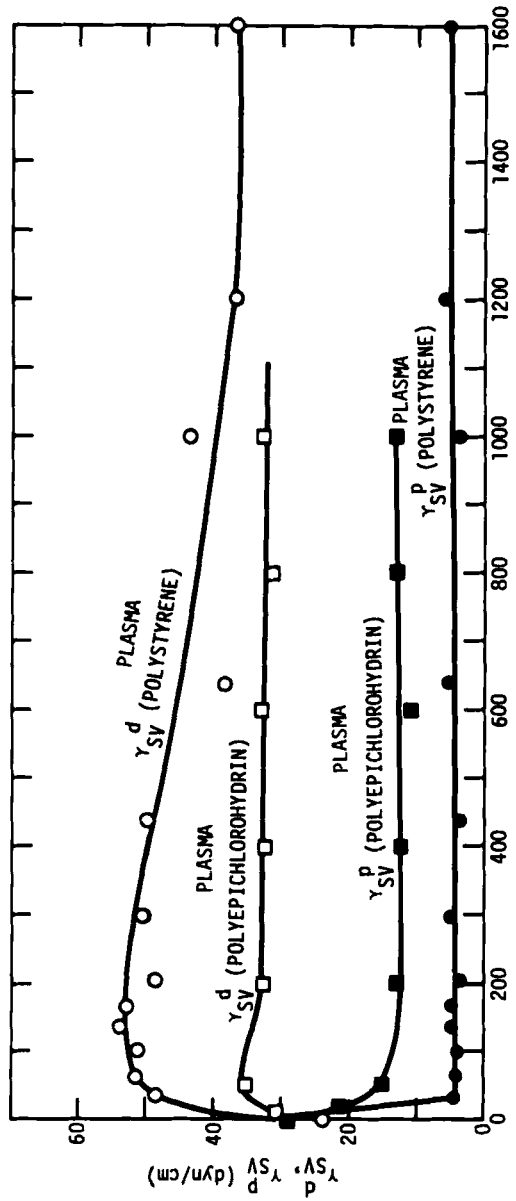

FIG. 8. Effect of film thickness on the surface energy components of plasma polystyrene and polyepichlorohydrin films on FPL-etched Al 2024-T3.

negative. This indicates a breakdown in the two-parameter model for solid-liquid interactions and results in the apparent high γ_{SV}^{d} values calculated. As yet this model has not been extended to include the effects of surface irregularity, but the experimental contact angle measurements can be correlated with the properties for nonuniform surfaces discussed by Adamson [26]. In Table 2 it is found that the contact angles of the higher surface tension liquids on PPS display increasingly larger values for thinner films. The contact angles of lower surface tension liquids, however, are nearly independent of film thickness. In Fig. 9, contact angle vs PPS film thickness is plotted for the four highest surface tension test liquids. As in the previous calculations of the surface energies, a leveling off in contact angle is noted for films greater than ~600 Å. These observations of thin PPS films on FPL-etched Al correlate with predictions of the effect of surface roughness or porosity on contact angle [26]. Generally it is found that if a liquid displays a large contact angle on a smooth surface, then roughening the surface will increase that angle. If, however, the contact angle is small on the smooth surface, it will decrease with increased roughness. Qualitatively, this is found for the case of thin PPS films on etched Al.

On FPL-etched Al, SEM studies reveal several types of roughness [27]. The predominant features are etch pits in the range ~1 to 10 μm in diameter and much smaller ones of the

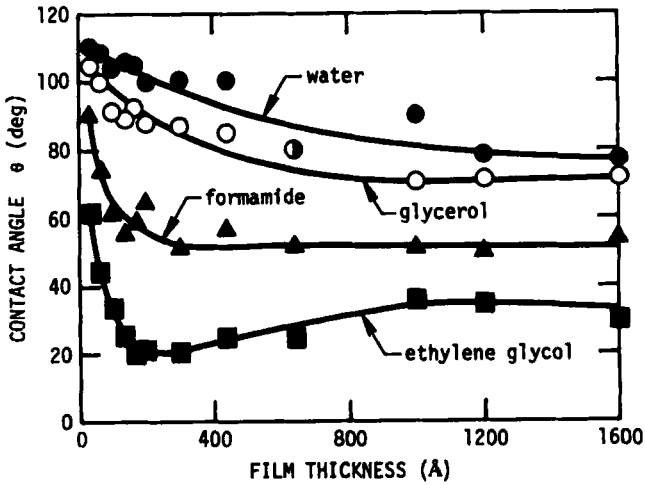

FIG. 9. Dependence of contact angle on the film thickness of plasma polystyrene deposited on FPL-etched Al 2024-T3.

order of ~100 Å. Evidence of the importance of these etch pits on the growth of plasma films has been given by Niinomi and co-workers [9]. They show that on certain electropolished aluminum substrates where the surface is covered by small etch pits ~100 Å in diameter, that plasma polyethylene deposits as a rough film. Growth of these rough films appears to be nucleated in the small etch pits where polymer semispheres develop and finally coalesce to form a continuous film. Larger pits or irregularities do not seem to cause rough films to grow. In the present work, however, we are concerned with an effect which increases as the PPS film thickness decreases down to the thinnest studied of ~37 Å. It therefore seems likely that it is the roughness of the original FPL-etched substrate and not that resulting from polymer deposition which is responsible for the observed effect.

Initially, FPL-etched Al is of such high surface energy that all the test liquids display nearly zero contact angle in spite of the surface roughness caused by the etch pits. If we consider, however, the deposition of a thin layer of low-energy material such as PPS which is nucleated in the etch pits, then the surface becomes a composite of open etch pits containing PPS and a background of FPL-etched Al. At this stage those liquids which show a large contact angle on PPS will not be able through capillary action to interact with the PPS in the pitted areas. Those liquids with a low contact angle on PPS should either decrease their contact angles or stay the same. The etch pits therefore act toward the high surface tension liquids as open areas where $\gamma_{SV} = 0$ and $\cos \theta = -1$. Considering the above growth mechanism, the contact angle data suggest that as the PPS film grows the etch pits fill, decreasing the amount of area where $\cos \theta = -1$ until at ~600 Å the pits disappear, resulting in a surface with normal properties. In addition, for PPS films thinner than those studied, the contact angles in Fig. 9 must at some thickness below monolayer coverage begin to decrease to the values for the virgin substrate. Examples of this kind of behavior are known for water contact angles on paraffined metal screens, certain fabrics, and in biological systems [26], but the scale of irregularity in the present work is much smaller.

Unlike PPS, no contact angle increase is found for thinner films of PPE on FPL-etched Al. Whether this is a result of a different growth mechanism or to the somewhat more polar character of this polymer is not known. More work is underway in studying wettability behavior as it is affected by the substrate and the type of monomer polymerized.

In order to evaluate the adhesive and cohesive properties of plasma films, overlap bonds representing the system Al/plasma polymer/epoxy adhesive/plasma polymer/Al were prepared in

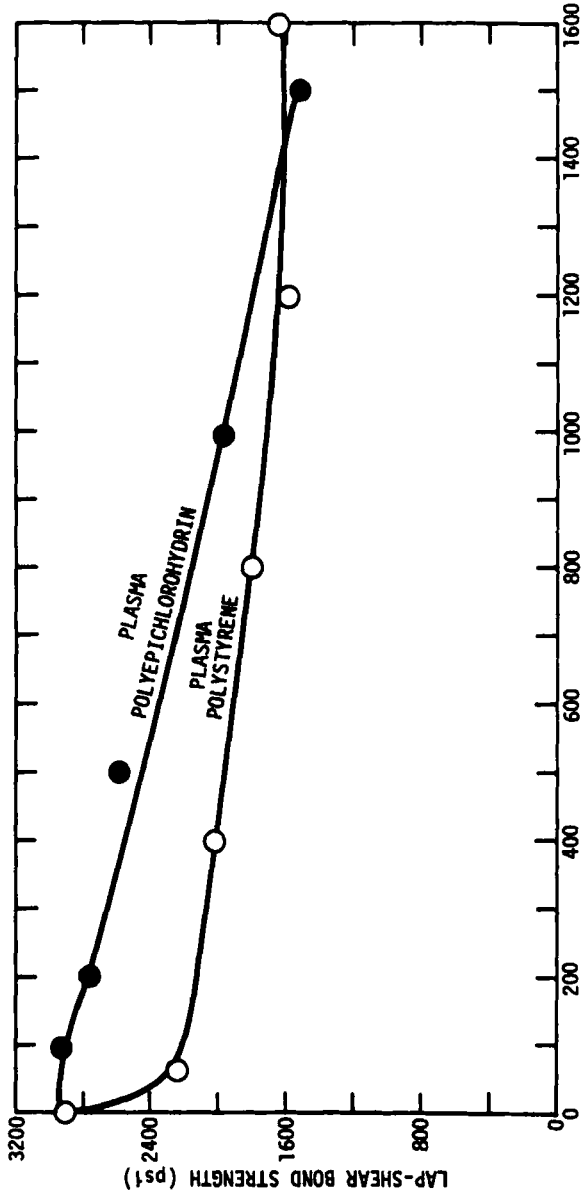

FIG. 10. Effect of plasma film thickness on the lap-shear bond strength of adhesively bonded FPL-etched Al 2024-T3 with HT-424 epoxy-phenolic adhesive.

which the thickness of the plasma polymer film was varied. In Fig. 10 the results of this study are given, where tensile shear strength is plotted vs plasma polymer film thickness. For bonds prepared without a plasma coating, failure occurs almost exclusively in the epoxy adhesive, giving a ~3000 psi bond strength. As the thickness of the PPS or PPE film is increased up to ~1500 Å, the fraction of cohesive failure in the adhesive decreases to almost zero and the bond strength drops to ~1600 psi. The exact location of failure in these bonds is difficult to determine. Qualitatively, it is observed that the discoloration caused by the thicker plasma films on Al 2024-T3 can be seen on the bond fracture surfaces, which would eliminate extensive failure near the Al/plasma polymer interface. Failure is therefore believed to occur near the plasma polymer/epoxy adhesive interface. Although the ~1600 psi bond strength is still relatively high, more work is needed to improve the adhesion between the plasma polymer and adhesive. More importantly, however, the plasma films appear to be very strongly bonded to the etched Al surface.

CONCLUSIONS

The main conclusions of the present work are the following:

1. Precise film deposition rates for glow discharge polymers on metallic substrates can be determined by the ellipsometric method.
2. For transparent plasma films the index of refraction can also be calculated.
3. The polar and dispersion surface energy character of plasma polymer films can be isolated by application of a two-parameter surface energy model to the analysis of wettability data.
4. In certain cases, wettability measurements are sensitive to the presence of surface roughness caused by substrate topology or the mechanism of plasma film growth.
5. Lap-shear bond studies indicate plasma polymer films possess strong adhesion to etched metallic substrates.

ACKNOWLEDGMENTS

The authors acknowledge helpful discussions with Dr. T. Smith concerning the ellipsometric calculations and the technical assistance of L. W. Crane.

REFERENCES

[1] L. V. Gregor, IBM J. Res. Dev., 12, 140 (1968).
[2] A. M. Means, Thin Solid Films, 3, 201 (1969).
[3] J. R. Hollahan and T. Wydeven, Science, 179, 500 (1973).
[4] B. Suryanarayanan, J. J. Carr, and K. G. Mayhan, J. Appl. Polym. Sci., 18, 301 (1974).
[5] L. F. Thompson and G. Smolinsky, Ibid., 16, 1179 (1972).
[6] F. Y. Chang, M. Shen, and A. T. Bell, Ibid., 17, 2915 (1973).
[7] "Plasma Technique For Osmosis Membranes," Chem. Eng. News, p. 47, (September 23, 1974).
[8] D. H. Kaelble, Proceedings of the 23rd International Congress of Pure and Applied Chemistry, Vol. 8, Butterworths, London, 1971, pp. 265-302.
[9] M. Niinomi, H. Kobayashi, A. T. Bell, and M. Shen, J. Appl. Polym. Sci., 18, 2199 (1974).
[10] M. Niinomi, H. Kobayashi, A. T. Bell, and M. Shen, J. Appl. Phys., 44, 4417 (1973).
[11] H. Yasuda and C. E. Lamaze, J. Appl. Polym. Sci., 15, 2277 (1971).
[12] H. W. Eichner and W. E. Schowalter, Forest Products Laboratory Report No. 1812, Madison, Wisconsin, May 1950.
[13] F. L. McCrackin, E. Passaglia, R. R. Stromberg, and H. L. Steinberg, J. Res. Nat. Bur. Stand., A67, 363 (1963).
[14] "Proceedings of the Symposium on Recent Developments in Ellipsometry," N. M. Bashara, A. B. Buckman, and A. C. Hall, eds., Surf. Sci., 16, (1969).
[15] R. J. King, Vacuum, 22, 493 (1972).
[16] F. L. McCrackin, Nat. Bur. Stand. Tech. Note 479 (April 1969).
[17] D. H. Kaelble, Physical Chemistry of Adhesion, Wiley, New York, 1971.
[18] D. H. Kaelble, P. J. Dynes, and E. H. Cirlin, J. Adhes., 6, 23 (1974).
[19] M. A. Barret and A. B. Winterbottom, First International Congress on Metallic Corrosion, London, 1961, Butterworths, London, 1962.
[20] C. A. Fenstermaker and F. L. McCrackin, Surf. Sci., 16, 85 (1969).
[21] G. M. Kline, Analytical Chemistry of Polymers, Part III, Wiley-Interscience, New York, 1962.
[22] A. Bui, H. Carchano, J. Guastavino, D. Chatain, P. Gautier, and C. Lacabanne, Thin Solid Films, 21, 313 (1974).
[23] W. W. Knickmeyer, B. W. Peace, and K. G. Mayan, J. Appl. Polym. Sci., 18, 301 (1974).

[24] R. A. Connell and L. V. Gregor, J. Electrochem. Soc., 112, 1198 (1965).
[25] L. F. Thompson and K. G. Mayan, J. Appl. Polym. Sci., 16, 2317 (1972).
[26] A. W. Adamson, Physical Chemistry of Surfaces, 2nd ed., Wiley-Interscience, New York, 1967.
[27] R. L. Patrick, ed., Treatise on Adhesion and Adhesives, Vol. 3, Dekker, New York, 1973.